Journal of Engineering and Applied Sciences 13 (24): 10323-10333, 2018
ISSN: 1816-949X

Effect of Atmospheric Stability Conditions on the Dispersion and Deposition Rates of Particulate Matter on the Surface of High Voltage Insulators

Amer D. Z. Albdiri
Department of Chemical Engineering, College of Engineering,
University of Al-Qadisiyah, Al-Diwaniyah, Iraq

Abstract: Recent frequent power outages of a 400/132 kVA substation near Al-Diwaniyah city coincided with an expansion of the brick industry in the same area have called for extensive study to investigate the probable effect of stack emission from brick factories on the occurrence of high voltage insulator flashover. Experimental and theoretical investigations have been conducted to predict the dispersion and deposition of Particulate Matters (PM) released from the neighboring brick factories within the area of study. Measurements of relevant airborne pollutants; Carbon dioxide (CO_2), Volatile Organic Carbon (VOC), Total Organic Carbon (TOC) and PM at 2000 m from the boundary of the brick factories were taken in the opposite direction of the prevailing wind (upwind location) and considered as reference readings. Downwind measurements were taken each 250 m from the boundary of the brick factories up to the 400/132 kVA substation. Meteorological data were measured to evaluate its effect on the dispersion and deposition rates of PM. The Gaussian dispersion model was adopted to simulate the local air pollution and the characteristic distance for PM was determined. Obtained results show that atmospheric stability conditions play a major role in determining the values of the dispersion and deposition rates of PM on the surface of the high voltage insulators and consequently the occurrence of flashover during wet atmospheric conditions (fog and mist). Deposited layer thickness varies in order of magnitudes when atmospheric stability changes from moderate unstable conditions (class B) to stable conditions (class F).

Key words: Pollution dispersion model, pollution deposition, pollution related flashover, atmospheric stability, determined, boundary of the brick

INTRODUCTION

The dispersion of industrial air pollutants depends on many factors, pollutant type and emission rate, wind speed and direction, stack height, plume rise and atmospheric stability conditions. Axial (downwind), horizontal (crosswind) and vertical dispersion of pollutants in air is promoted by advection, eddies and random perturbations of wind, respectively. Particulate Matter (PM) and black carbon (Soot) are considered the most adverse pollutants for high voltage insulators. Outdoor high voltage insulators, used in high voltage transmission lines and electrical power substations are likely susceptible to obstruct airflow and produce turbulence which cause an aerodynamic catch (deposition) of particles on its surface. The rate of deposition of the PM on the surface of the high voltage insulator depends on the size and concentration of particles, the geometry of the insulator and the airflow velocity. The thickness of the deposited layer depends on the continuous deposition of the particles and the blowing of loose particles due to the cleaning effect of wind (Amarh, 2001). Rain (during rainy season) also washes away part of the deposited layer. Jiang *et al.* (2017) proposed a mathematical model to relate the rainfall intensity and insulator self-cleaning capability. The model was reported to predict surface pollution characteristics and provide power system operators the ability to decide when initiate insulator cleaning. The process of deposition and self-cleaning continues to form a thin layer of solid deposit on the surface of the insulator. Moistening this layer by fog, mist, light rain usually leads to a thin conducting layer on the surface of the insulator (Zhicheng *et al.*, 2015; Zhang *et al.*, 2008; Lloydand and Schneider, 1982). A leakage current is then initiated and water starts to evaporate due to heat accumulated in the conducting layer. Then dry bands will be developed and localized arcing may take place and lead to a flashover. Therefore, a contamination monitoring becomes a necessity to predict the pollution related flashovers. Modelling of the relationship between climate variables and the risk of failure associated with the leakage current was investigated by Sierra *et al.* (2015). Finite Element Method (FEM) was implemented by Gencoglu and Cebeci

(2008) to determine the potential distribution on the surface of the insulator. Air pollution models (dispersion models) are widely used to map the spread of pollutants released from industrial sources and predict rates of diffusion based on meteorological parameters (Macdonald, 2003; Jacimovski *et al*., 2017). AICE and CCPS (1996) suggested the following equation to determine the worst conditions mean pollutant concentration downwind of a point source in Eq. 1:

$$C_{wc} = \frac{10^9 Q}{U H_{wc} W_{wc}} \quad (1)$$

Where:

C_{wc} = Worst Conditions pollutant concentration ($\mu g/m^3$)
Q = Source emissions rate of particulate (kg/sec)
U = Worst conditions wind speed at height (z = 10 m), usually 1 m/sec
H_{wc} = Worst Conditions Cloud depth, usually assumed 50 m
W_{wc} = Worst Conditions Cloud width, usually assumed (0.1X) where X is the distance from source

Atmospheric stability conditions play a major role in pollutants dispersion scheme. Conning, fanning, fumigation, lofting, trapping and looping are common dispersion behaviors of pollution and temperature lapse rate dependent. However, the transport of pollutants from their sources to contaminated destinations is not the only mechanism of contamination. The deposition of pollutants on the surfaces of destinations is another major process of contamination. The "big leaf" model is widely used to estimate the deposition of pollutants. The deposition rate can be determined using the following Eq. 2 (Lagzi *et al*., 2004; Meszaros *et al*., 2009a, b):

$$V_d = \frac{1}{R_a + R_b + R_c} \quad (2)$$

Where:

V_d = Pollutant deposition velocity
R_a, R_b, R_c = Aerodynamic, boundary-layer and canopy resistances, respectively

Pollutant deposition may take place under dry or wet conditions. The flashover of insulator under haze-fog condition was reported by Guo *et al*. (2016) to be a special kind of pollution flashover as the flashover voltage increases with the increase of the particle size but decreases with the increase of fog-water conductivity. Guo *et al*. (2016) found that salt fog deposit increases the insulator surface conductivity and degrades the flashover performance of the insulator.

Modeling of pollutant dispersion and deposition using commercial or in-doors models can help researchers to predict when a critical thickness of conducting layer reached and an action is needed. However, as meteorological variables play crucial role in both dispersion and deposition processes, investigations should consider atmospheric fluctuations and wind perturbations to select the proper atmospheric stability category (A-F class). These six stability classes range from very unstable conditions A to moderately stable conditions F. Stability class is a strong function of wind speed, sun elevation and cloud cover (Sriram *et al*., 2006; Turner, 1997). Gaussian Model among many models is considered the most commonly used for predicting pollution dispersion (Lushi and Stockie, 2010). However, Fay and Golomb (2012) indicated that Gaussian model may overestimate ground concentration of pollutant up to two times measured values. Zhicheng *et al*. (2015) simulated the air pollution and its relation to heavy haze weather, based on the daily average concentration of pollutants and using numerical prediction method. To the best knowledge of the researcher, few researchers have related theoretical and experimental researches to predict and simulate the pollutant dispersion and deposition schemes. This research may be considered a field study to trace the transport of Particulate Matter (PM) emitted from a brick industry area located 5 km from a 400/132 KVA substation. Field measurements of meteorological parameters and air and soil concentrations of pollutants were carried out and compared to modeling results.

MATERIALS AND METHODS

Area of study: The area of study is shown in Fig. 1, located to the North-West of the Dewaniyah City. The brick factories are 5 km to the North of the 400/132 KVA substation. The whole area is characterized as a rural and flattened-terrain area. The Prevailing winds in the area of study are North to North-West directions and 4-10 m/sec speed. The brick factories are 12 factories of a daily production of 48000 bricks each. The daily consumption of heavy oil fuel is 7000 L each.

Mathematical modeling and analysis: Air dispersion models are widely used to evaluate the consequences of accidental releases of chemicals and determine the impacted area. Pollutant concentrations are temporally and spatially tracked and estimated. Currently, the most widely used model is the Gaussian-Plume Model (Carbon, 2004).The Gaussian-Plume model is based on steady-state assumption, therefore, it is only spatial-dependent model. Figure 2 schematically represents a typical plume dispersion scheme.

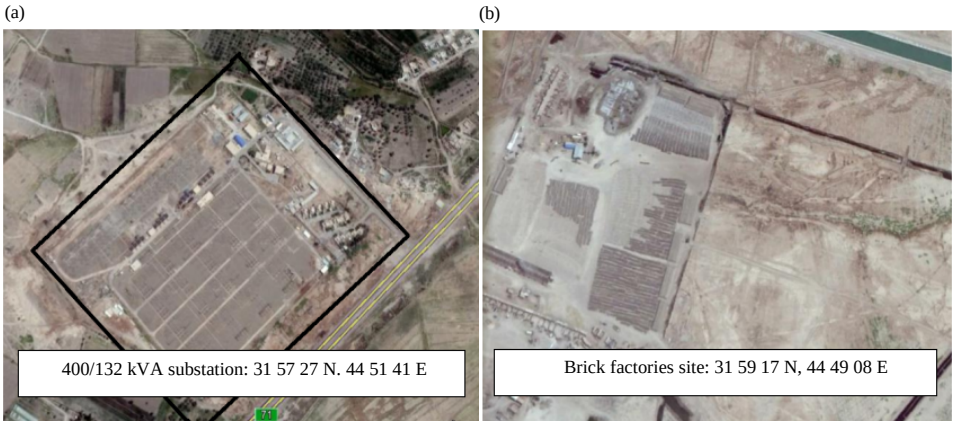

Fig. 1a, b): Area of study

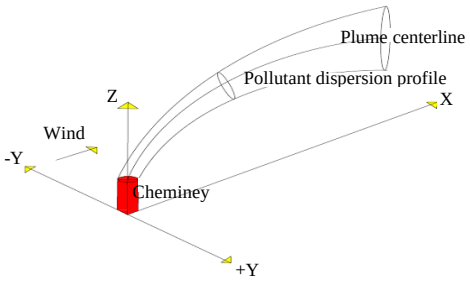

Fig. 2: Typical plume dispersion scheme

The Gaussian-plume model is based on the diffusion equation and can be mathematically expressed by the following general Eq. 3 (Macdonald, 2003):

$$C_{(x,y,z)} = \frac{Q}{2\pi U\sigma_y\sigma_z}\exp\left(-\frac{y^2}{2\sigma_y^2}\right)$$
$$\left[\exp\left(-\frac{(z-H)^2}{2\sigma_z^2}\right)+\exp\left(-\frac{(z+H)^2}{2\sigma_z^2}\right)\right] \quad (3)$$

Where:

Q = Source emissions rate of particulate (gm/sec)
U = Wind speed (m/sec)
σ_y = Crosswind dispersion coefficient (m)
σ_z = Vertical dispersion coefficient (m)
H = Effective stack height (m) = $H_s+\Delta H$, H_s stack height (m)
ΔH = Plume rise (m)

$$\Delta H = \frac{21.425F^{0.75}}{U} \text{ for } F \le 55 \text{ m}^4/\text{s}^3 \quad (4)$$

$$\Delta H = \frac{38.71F^{0.6}}{U} \text{ for } F \ge 55 \text{ m}^4/\text{s}^3 \quad (5)$$

$$F = gV_sd^2(T_s - T_a)/4T_s \quad (6)$$

Where:

F = Bouncy flux
V_s = Stack exit velocity (m/sec)
d = Top inside stack diameter (m)
T_s = Stack gas temperature (K)
T_a = Ambient temperature (K)
g = Gravity (m/s^2)
σ_y and σ_z = Strong functions of downwind distance (x)

Atmospheric stability and can be determined from specific monographs or empirical equations. The downwind concentration profiles and crosswind and vertical dispersion envelopes were estimated using Microsoft Excel program. The source of pollution was assumed a point source despite that we have 12 brick factories emitting pollutants. The reason behind this assumption is the relatively large distance between a factory and others. Field observations show that plume paths of the 12 brick factories were almost non-interacting at the initial phase of emission. It was observed that plumes were interfered at the midway of their paths. Therefore, it was found reasonable to sum the estimated concentrations of all plumes at the destination point (400/132 kVA substation).

The arrival of the polluted air to the substation causes the deposition of part of the pollutant onto the surface of the insulators. The initial deposition rate of pollutants onto the surface of the insulator was found to be high as the insulator is clean and then after a month, it decreases as the capture efficiency drops considerably. The 30 days exposure is a standard exposure time for Equivalent Salt Deposit Density (ESDD) (Zhicheng *et al*., 2015; Vosloo, 2002). The deposition rate of pollutants is a strong dependent of insulator surface area, surface roughness, aerodynamic profile of the insulator, the type

Table 1: Air sampling details

Sample No.	Location	Date of sampling	Time of sampling	Weather conditions (°C, m/sec)
1	2000 m upwind (control point)	3/4/2017 repeated 1/5/2017	10.00 morning	T: 28.4, sunny day, wind speed: 4
			10.00 morning	T: 29.6, sunny day, wind speed: 5
2	Brick factories site	3/4/2017 repeated 1/5/2017	11.00 morning	T: 28.9, sunny day, wind speed: 4
			11.00 morning	T: 29.6, sunny day, wind speed: 5
3	250 m downwind	1/5/2017	12.35 noon	T: 30.4, sunny day, wind speed: 5
4	500 m downwind	1/5/2017	1.51 noon	T: 30.5, sunny day, wind speed: 5
5	750 m downwind	1/5/2017	3.15 noon	T: 31.1, sunny day, wind speed: 5
6	1000 m downwind	4/4/2017 repeated 5/5/2017	9.32 morning	T: 26.8, slight clouds, wind speed: 5
			9.30 morning	T: 29.4, sunny day, wind speed: 5
7	1250 m downwind	5/5/2017	10.40 morning	T: 29.8, sunny day, wind speed: 5
8	1500 m downwind	5/5/2017	12.05 noon	T: 30.1, sunny day, wind speed: 5
9	1750 m downwind	5/5/2017	1.23 noon	T: 30.4, sunny day, wind speed: 5
10	2000 m downwind	4/4/2017 repeated 5/5/2017	12.55 noon	T: 27.1, slight clouds, wind speed: 5
			2.35 noon	T: 30.8, sunny day, wind speed: 5
11	Substation site	20/4/2017 repeated 22/5/2017	9.52 morning	T: 29.3, sunny day, wind speed: 4
			12.10 noon	T: 34, sunny day, wind speed: 5

Table 2: Soil sampling details

Sample No.	Location	Date of sampling	Time of sampling	Weather conditions (°C, m/sec)
1	2000 m upwind (control point)	3/4/2017	10.10 morning	T: 28.4, sunny day, wind speed: 4
2	Brick factories site	3/4/2017	11.15 morning	T: 28.9, sunny day, wind speed: 4
3	1000 m downwind	4/4/2017	9.48 morning	T: 26.8, slight clouds, wind speed: 5
4	2000 m downwind	4/4/2017	1.55 noon	T: 27.3, slight clouds, wind speed: 5
5	Substation site	20/4/2017	10.10 morning	T: 29.3, sunny day, wind speed: 4
		repeated 22/4/2017	12.00 noon	T: 29.9, sunny day, wind speed: 4

and concentration of the pollutant, humidity and wind speed (Haberecht, 2008). The deposition rate is estimated using the following formulas (Klassen *et al*., 1999):

$$N = UC_{\alpha}\eta \quad (7)$$

$$\eta = \frac{D_t U_i S}{F} = D_t U_i S \quad (8)$$

Where:

N = Deposition rate (g/m^{2}sec)
U = Wind velocity (m/sec)
Cα = PM concentration (g/m^3)
η = Impact efficiency of insulator
D_t = Insulator diameter (m)
U_i = Particle velocity (m/sec)
S = PM diameter (m)
F = Unit flux of air arriving per unit area at 1 m/sec = 1

The deposit rate onto the surface of insulator was related to dispersion model results and corresponding values were estimated using Microsoft Excel program. Then, the thickness of the pollutant layer was estimated for each case and an investigation of the effect of atmospheric conditions on its thickness was carried out and plotted.

Field measurements and experimental work

Field measurements: Eleven air and five soil samples were collected during the period extended from April 3rd-May 22nd, 2017 as shown in Table 1 and 2. Ambient weather parameters were also measured and recorded for all air and soil samples. Volumetric gas filters were used for the collection of air samples and all samples were drawn at height 1.5 m above ground level. Soil samples were extracted using clean and dry jars (piece of PVC pipe) from randomly selected points along the path extended from the brick factories to the substation. The depth of the extracted samples was 20 cm. Air and soil samples were brought to laboratory for chemical and physical analysis.

Laboratory analysis: All field collected samples (air and soil) were brought to laboratory at the same day of collection for chemical and physical analysis. pH, VOC, TOC, CO_2 and metals (Pb, Mn, Cd, Ni) were determined for all samples. pH meter (3320 Jenway), spectrophotometer (Shimadzu 1280), atomic absorption spectrophotometer (Shimadzu AA-7000), Gas Chromatography (GC-2025) and portable photometer (PhotoFlex) were used for the chemical and physical analysis following standard methods of analysis. Handheld particle counter (Met One) was used to determine $PM_{2.5}$, PM_{10}, TSP. Battery powered mobile Gasmet analyzer was also used to measure gaseous air pollutants (SO_2, NO_2, CO, O_3, CH_4).

RESULTS AND DISCUSSION

Theoretical analysis: Vertical and crosswind PM dispersion profiles (μg/m^3) were calculated under three atmospheric stability cases (moderately unstable conditions (class B), neutral conditions (class D) and stable conditions (class F)) using Gaussian dispersion model. The obtained results for each class of atmospheric stability are presented in two sections. First section expresses the profiles from emission source up to

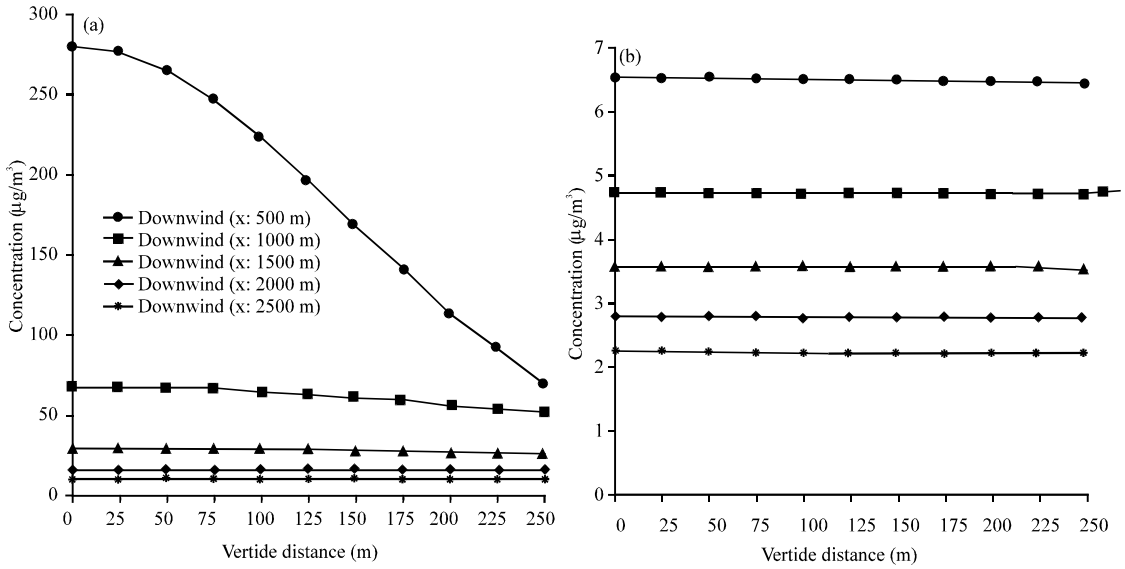

Fig. 3: PM verticle concentration profile (µg/m^3) downwind distance extended between source and destination points under moderately unstable atmospheric conditions (class B); a) PM verticle concentration profile (µg/m^3) for 1st half downwind distance and moderately unstable atmospheric condition and b) PM verticle concentration profile for 2nd half downwind distance and modaretely unstable atmospheric condition

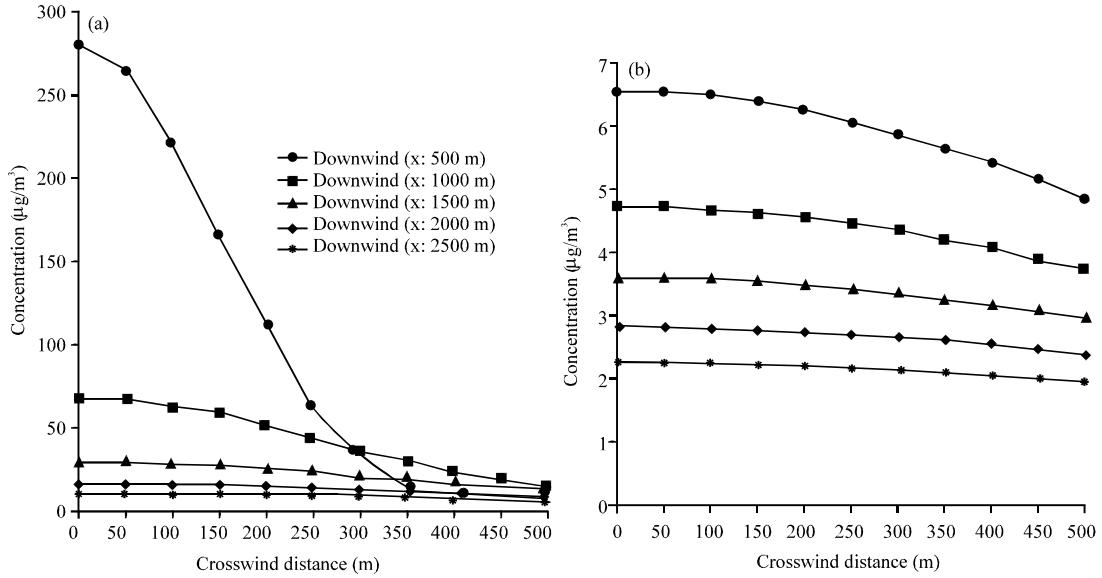

Fig. 4: PM crosswind concentration profile (µg/m^3) downwind distance extended between source and destination points under moderately unstable atmospheric conditions (class B); a) PM crosswind concentration profile (µg/m^3) for 1st half downwind distance and modaretely unstable atmospheric conditions and b) PM crosswind concentration profile (µg/m^3) for 2nd half downwind distance and modaretely unstable atmospheric conditions

mid-distance while the second section expresses the final part of the dispersion distance. Figure 3 shows the vertical concentration (µg/m^3) profiles of downwind distance extended between source (brick factories site) and destination (substation site) points under moderately unstable atmospheric conditions (summer day with some broken clouds). Figure 3 is presented in two sections; the first section represents the first 2500 m distance from source point up to the mid-distance (Fig. 4). The vertical concentration profile for each 500 m is shown. It clearly shows that the concentration profile of the first 500 m rapidly declines from about 280 µg/m^3 at the centerline of

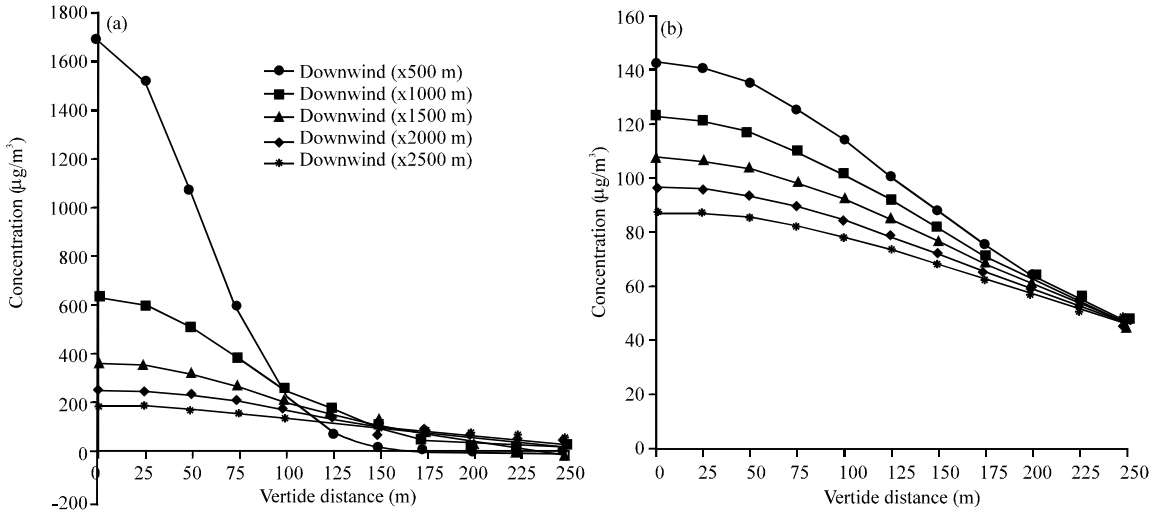

Fig. 5: PM verticle concentration profile (µg/m^3) downwind distance extended between source and destination points under Neutral atmospheric conditions (class D); a) PM verticle concentration profile for 1st half downwind distance and neutral atmospheric conditions and b) PM verticle concentration profile (µg/m^3) for 2nd half downwind distance and neutral atmospheric conditions

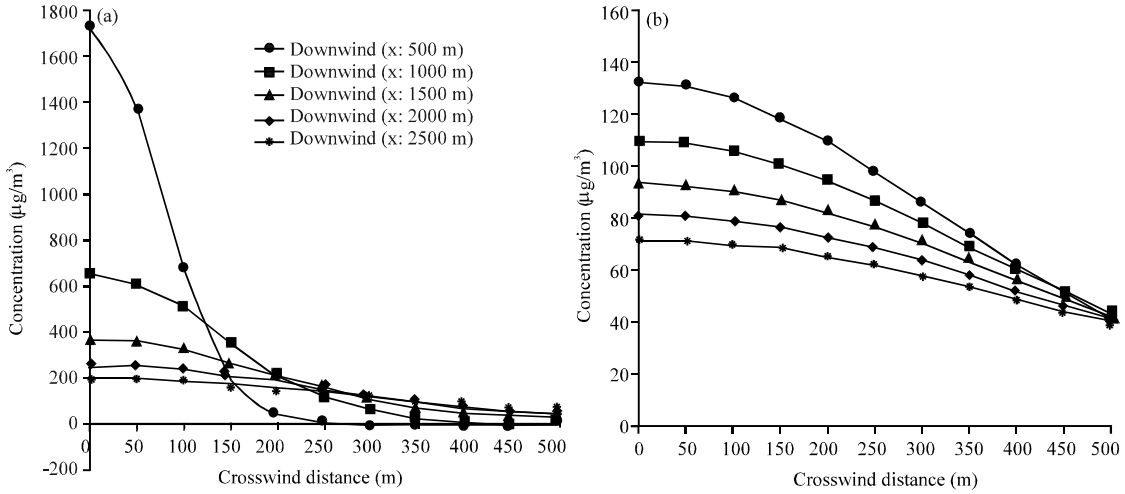

Fig. 6: PM crosswind concentration profile (µg/m^3) downwind distance extended between source and destination points under neutral atmospheric conditions (class D); a) PM crosswind concentration profile (µg/m^3) for 1st half of downwind distance and neutral atmospheric conditions and b) PM crosswind concentration profile (µg/m^3) for 2nd half of downwind distance and neutral atmospheric conditions

the plume to about 70 µg/m^3 at 250 m vertical distance above the centerline. However, it was found that concentration profiles at distances 1000 , 1500 , 2000 and 2500 m flatten indicating insignificant vertical profile decay. The results demonstrate a gradual regression of concentration in both centerline and vertical directions. The second half distance of plume path follows the same trend of concentration behavior obtained at far distances of the first part where the centerline concentration reached a minimum of about 2 µg/m^3 at the substation site (Fig. 5 and 6).

Figure 4 depicts the crosswind concentration profiles obtained along the plume path under the moderately unstable atmospheric conditions (class B) and also sectioned in two parts (near source (0-2500 m) and near destination (2500-5000 m) parts). The crosswind concentration profile at 500 m downwind station exhibits

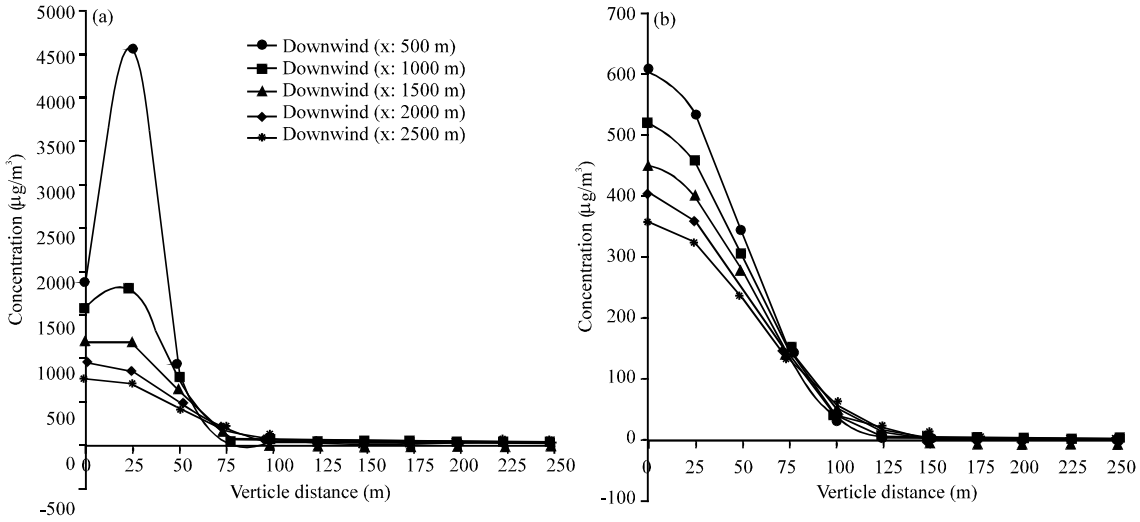

Fig. 7: PM verticle concentration profile (µg/m^3) downwind distance extended between source and destination points under stable atmospheric conditions (class F); a) PM verticle concentration profile (µg/m^3) for 1st half of downwind distance and stable atmospheric conditions and b) PM verticle concentration profile (µg/m^3) for 2nd half of downwind distance and stable atmospheric conditions

a rapid decay from centerline concentration of 280 µg/m^3 to about zero concentration at 400 m distance from centerline. Concentration crosswind profiles at further downwind stations show smooth decline from center to about 450 m lateral distance. It can be concluded that moderately unstable atmospheric conditions result in fast dispersion of PM near the source point (brick factories site) and rapid downwind concentration decay. Therefore, the expected PM deposition rate at the substation site is a minimum.

Figure 5 and 6 demonstrate vertical and crosswind PM concentration profiles under neutral atmospheric conditions (cloudy summer day with lower air velocity than prevailing wind speed, Class D). The results show significant differences in concentration values from that under moderately unstable atmospheric conditions. The centerline concentration at 500 m downwind distance is as high as 1600 µg/m^3 in comparison to 280 µg/m^3 for moderately unstable conditions. However, it was noticed that high decay rate of both vertical and crosswind concentration profiles (the concentration drops from 1600 µg/m^3 to about zero concentration at 100 m vertical distance and 200 m crosswind distance). This results in narrower plumes than those under unstable atmospheric conditions. Therefore, it can be concluded that lower wind speeds result in lower vertical and crosswind dispersion rates and higher concentrations values downwind stations of plume path. The concentration of PM at the substation site under neutral atmospheric condition was found to be 37 times higher than that of unstable atmospheric conditions. This may cause higher deposition rates of PM on the surface of high voltage insulators (Fig. 7 and 8).

Figure 7 and 8 detail the profiles of both vertical and crosswind dispersion of PM along the plume path under stable atmospheric conditions (cloudy and low wind speed). Figure 7 shows the vertical dispersion profiles of PM. It was found that at downwind distance of 500 m, the vertical concentration profile rises from about 1600 µg/m^3 at the centerline of the plume to about 4000 µg/m^3 at a vertical distance of 25 m and then sharply drops to zero concentration at 75 m. The interpretation of this unexpected behavior may be due to eddies and local circulatory flow. The high concentration difference between this vertical distance and the centerline will lead to backward dispersion and further turbulence. However, beyond the 500 m downwind station, the vertical concentration profile gradually concaves and rounds to become declining profile. The minimum centerline concentration of PM at the substation site under stable condition was found to be 375 µg/m^3 which is 5 times higher that of neutral atmospheric conditions. This again confirms the fact that lower wind speeds and increasing the cloudiness result in lower dispersion rates of PM along plume paths and consequently narrow plume cone. The expected deposition rate at the substation site under the stable atmospheric conditions is the highest on the surfaces of the high voltage insulators.

The dependence of the PM above ground concentration on the wind speed is clearly illustrated in

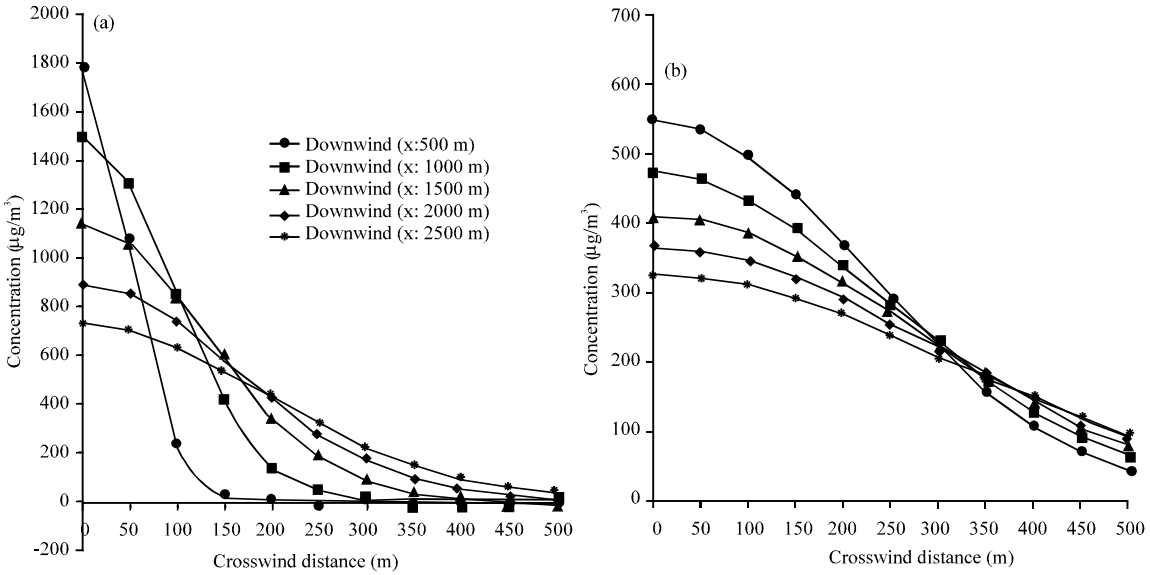

Fig. 8: PM crosswind concentration profile (µg/m^3) downwind distance extended between source and destination points under stable atmospheric conditions (class F); a) PM crosswind concentration profile (µg/m^3) for 1st half of downwind distance and stable atmospheric conditions and b) PM crosswind concentration profile (µg/m^3) for 2nd half of downwind distance and stable atmospheric conditions

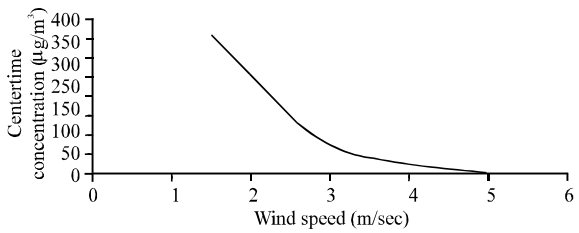

Fig. 9: PM above ground concentration dependence on atmospheric conditions (wind speed and cloud density)

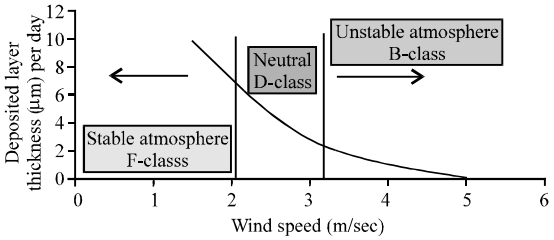

Fig. 10: PM deposition rate dependence on atmospheric stability (wind speed and cloud density)

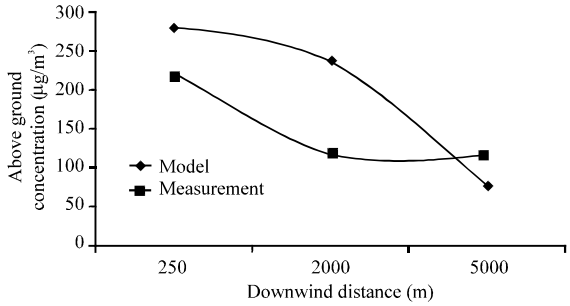

Fig. 11: Comparison of model results and field measurements of PM concentration (wind speed and cloud density)

Fig. 9 where the rapid decline of concentration is distinctly shown. The concentration drops from about 360 µg/m^3 at wind speed of 2 m/sec to about 2 µg/m^3 at wind speed of 5 m/sec. The interpretation of this sharp drop in centerline concentration is due to high dispersion rates in both vertical and crosswind directions at relatively higher wind speeds (atmospheric conditions tend to become unstable as wind speed increases). The lower wind speed and the increase of atmospheric cloudiness is expected to increase the agglomeration rate of the PM and consequently increases the effect of the gravity force on the PM. Low wind speed will also decrease the aloft of the PM and reduces the dispersion rate in both vertical and crosswind directions. Figure 10 demonstrates the dependence of the deposition rate of the PM on a surface of an insulator as a function of wind speed and atmospheric conditions (cloudiness). It is shown that below wind speed of 2 m/sec, the atmospheric condition is characterized as stable conditions and therefore, the

Table 3: Chemical analysis of air samples collected along the path of plume dispersion

Air sample No.	pH	VOC (%)	TOC (%)	CO2 (mg/m^3)	Pb (mg/m^3)	Mn (mg/m^3)	Cd (mg/m^3)	Ni (mg/m^3)
2000 m upwind	7.76	0.0054	0.0080	261.40	0.0019	0.0001	0.0003	0.0004
Brick factories site	6.80	0.0291	0.0339	732.46	0.0174	0.0069	0.0058	0.0052
250 m downwind	7.28	0.0302	0.0362	775.06	0.0103	0.0046	0.0039	0.0010
500 m downwind	7.49	0.0313	0.0358	756.07	0.0070	0.0032	0.0037	0.0031
750 m downwind	7.56	0.0293	0.0324	731.19	0.0072	0.0028	0.0031	0.0025
1000 m downwind	7.62	0.0215	0.0263	678.00	0.0065	0.0021	0.0024	0.0018
1250 m downwind	7.69	0.0187	0.0216	575.20	0.0058	0.0015	0.0017	0.0013
1500 m downwind	7.71	0.0170	0.0187	521.82	0.0049	0.0011	0.0013	0.0011
1750 m downwind	7.71	0.0112	0.0129	489.25	0.0031	0.0006	0.0008	0.0008
2000 m downwind	7.72	0.0082	0.0089	456.35	0.0029	0.0004	0.0005	0.0008
Substation site	7.21	0.0740	0.0846	132.01	0.0197	0.0088	0.0016	0.0031

Table 4: Chemical analysis of soil samples collected along the path of the plume

Soil sample No.	pH	VOC (%)	TOC (%)	Pb (mg/kg)	Mn (mg/kg)	Cd (mg/kg)	Ni (mg/kg)
2000 m upwind	-	0.0412	0.0474	0.0135	0.0071	0.001	0.0429
Brick factories site	5.64	1.71	2.226	0.0782	0.0507	0.0076	0.0143
1000 m downwind	6.01	0.6725	0.7020	0.039	0.0209	0.0046	0.0079
2000 m downwind	6.24	0.2035	0.2420	0.0242	0.0124	0.00025	0.0038
Substation site	5.89	1.557	1.6895	0.0207	0.0120	0.0013	0.0082

deposition rate of the PM is maximum. Between wind speed value (2-3.2) m/sec, the atmospheric conditions is characterized as neutral conditions and the deposition rate of the PM starts declining significantly with the increase of the wind speed. When the wind speed is above 3.2 m/sec, the deposition rate becomes very small. The low deposition rate is reflected in thin deposited layer of pollutant. However, the thickness of the deposited layer shown in Fig. 11 is not affected by the cleansing effect of winds.

Field and laboratory analysis: Air and soil samples were collected upwind and downwind the brick factories site at different distances using standard methods (Volumetric gas filters were used for the collection of air samples and all samples were drawn at height 1.5 m above ground level, soil samples were extracted using clean and dry jars at depth of 20 cm). Both gas filters and soil samples were taken to laboratory for chemical analysis. Results of air samples analysis are shown in Table 3. It is seen that all upwind samples (samples taken at a distance of 2000 m upwind the brick factories site) have minimum values of pollutants concentration to indicate that prevailing winds dominantly carry pollutants in a downwind direction. The results indicate that a noticeable concentration decline of most pollutants from the emission point (brick factories site) to destination point (substation site). However, the measurements have revealed the pollutant concentrations are higher than the expected values at the substation site (higher than the values of the pollutant concentration at the 2000 m downwind distance). The reason behind that is attributed to the recirculation and eddy flows within the substation site. The installations may disturb the downwind flow of atmospheric air to cause the recirculation and the eddy flows.

Table 5: Gaseous air pollutants concentration along the path of the plume using Gasmet device

Air sample No.	SO_2 (ppm)	NO_2 (ppm)	CO (ppm)	O_3 (ppm)	CH_4 (ppm)
Brick factories site	0.0	0.15	0.09	0.01	1.98
2000 m downwind	0.0	0.00	0.05	0.02	2.06
Substation site	0.0	0.20	0.07	0.00	1.87

Table 6: PM concentration profiles along the path of the plume under three different conditions of atmosphere

Air sample No.	$PM_{2.5}$ (µg/m^3)	PM_{10} (µg/m^3)	TSP (µg/m^3)
Brick factories site	33	147	219
2000 m downwind	8	69	117
Substation site	9	80	115

The results of the analysis of the soil samples are presented in Table 4. The results reflect that the concentration of pollutants inside the substation site is higher than the concentration of pollutants along the soil of the path of the plume, despite the continuous decrease of the concentration of the pollutants along the path of the plume. The area extended from the brick factories up the substation site is an agricultural area where irrigation and draining can significantly reduce the absorbed pollutants within the soil. The substation site was layered with coarse gravel which acts as a filter to concentrate the deposited pollutants at a depth of 20 cm below the surface of the ground as shown in Table 4.

Tables 5 and 6 show the concentration values of gaseous and PM pollutants at three points along the path of the plume (brick factories site, midway between brick factories and substation sites and the substation site) using handheld measuring devices (Handheld particle counter (Met One) was used to determine $PM_{2.5}$, PM_{10}, TSP. Battery powered mobile Gasmet analyzer was also used to measure gaseous air pollutants (SO_2, NO_2, CO, O_3, CH_4)). The obtained results confirmed the calculated results of the Gaussian dispersion model under neutral

atmospheric conditions. Fair agreement was noticed between the calculated PM concentration profile and the particle counter device measurements as shown in Fig. 11 and Table 6. Figure 11 shows that measurement's profile flatten at a specific value of concentration downwind the path of the plume while theoretical results show continuous decline of concentration to cross the measurement profile.

CONCLUSION

Emission of pollutants from brick factories, located 5000 m to the northwest of a 400/132 kVA substation was modeled using Gaussian dispersion model under three atmospheric stability conditions. The obtained results were compared with field measurements and observations. Fair agreement between the results of the modeling and that of the field measurements was obtained. Atmospheric stability conditions play major role in varying both vertical and crosswind dispersion rates. It was found that above ground pollutant concentration decays very fast under instability conditions of atmosphere, due to high vertical and crosswind dispersion rates. Stable atmospheric conditions can increase Particulate Matter (PM) agglomeration and consequently increases the rate of deposition of the PM. Higher deposition rates of the PM usually lead to a high thickness of deposit layer. The deposition rate of the PM on high voltage insulators results in high pollutant's layer thickness. The higher the thickness of pollutant layer, the higher flashover probability under wet conditions (humid atmosphere, fog and mist). However, rain normally washes the surface of the insulator and may lead to less probability of flashover.

ACKNOWLEDGEMENT

The researcher would like to thank assistant professor Hisham M. Majeed and Mr. Jabir A. Jabir for their support in performing field measurements and laboratory analysis.

REFERENCES

AICE. and CCPS., 1996. Guidelines for use of Vapor Cloud Dispersion Models. 2nd Edn., American Institute of Chemical Engineers, Center for Chemical Process Safety, Ann Arbor, Michigan, USA., ISBN:9780816907021, Pages: 271.

Amarh, F., 2001. Electric transmission line flashover prediction system. Ph.D Thesis, Arizona State University, Tempe, Arizona.

Carbon, B., 2004. Good Practice Guide for Atmospheric Dispersion Modeling. New Zealand Government-Ministry for the Environment, Wellington, Christchurch, South Island, New Zealand, ISBN:9780478189414, Pages: 142.

Fay, J.A. and D.S. Golomb, 2012. Energy and the Environment: Scientific and Technological Principles. 2nd Edn, Oxford University Press, New York, USA., ISBN:9780199765133, Pages: 366.

Gencoglu, M.T. and M. Cebeci, 2008. The pollution flashover on high voltage insulators. Electr. Power Sys. Res., 78: 1914-1921.

Guo, Y., X. Jiang, Y. Liu, Z. Meng and Z. Li, 2016. AC flashover characteristics of insulators under haze-fog environment. IET. Gener. Trans. Distrib., 10: 3563-3569.

Haberecht, P., 2008. Pollution deposition rates on insulator (HV) surfaces for use in atmospheric corrosivity estimation. Ph.D Thesis, University of Newcastle, Callaghan, Australia.

Jacimovski, S., S. Miladinovic, R. Radovanovic and V. Ilijazi, 2017. Use of gaussian mathematical model in the distribution of sulphur dioxide into the atmosphere from point source. Tech. Bull., 24: 157-162.

Jiang, Z., X. Jiang, Z. Zhang, Y. Guo and Y. Li, 2017. Investigating the effect of rainfall parameters on the self-cleaning of polluted suspension insulators: Insight from southern China. Energies, 10: 1-13.

Klassen, R.D., M. Tullmin and P.R. Roberge, 1999. Modeling of aerosol transport as an aid to corrosivity assessment. Proceedings of the International Conferences on Corrosion 99, April, 25-30, 1999, NACE International, San Antonio, Texas, ISBN:994891999, pp: 1-12.

Lagzi, I., D. Karman, T. Turanyi, A.S. Tomlin and L. Haszpra, 2004. Simulation of the dispersion of nuclear contamination using an adaptive Eulerian grid model. J. Environ. Radioact., 75: 59-82.

Lloydand, K.J. and H.M. Schneider, 1982. Insulation for power frequency voltage transmission line reference book (345 kV and above). Electric Power Research Institute, Palo Alto, California.

Lushi, E. and J.M. Stockie, 2010. An inverse Gaussian plume approach for estimating atmospheric pollutant emissions from multiple point sources. Atmos. Environ., 44: 1097-1107.

Macdonald, R., 2003. Theory and objectives of air dispersion modelling. Wind Eng., 2003: 1-27.

Meszaros, R., D. Szinyei, C. Vincze, I. Lagzi and T. Turanyi *et al*., 2009a. Effect of the soil wetness state on the stomatal ozone fluxes over hungary. Intl. J. Environ. Pollut., 36: 180-194.

Meszaros, R., I.G. Zsely, D. Szinyei, C. Vincze and I. Lagzi, 2009b. Sensitivity analysis of an ozone deposition model. Atmos. Environ., 43: 663-672.

Sierra, R.C., O. Oviedo-Trespalacios, J.E. Candelo and J.D. Soto, 2015. Assessment of the risk of failure of high voltage substations due to environmental conditions and pollution on insulators. Environ. Sci. Pollut. Res., 22: 9749-9758.

Sriram, G., N.K. Mohan and V. Gopalasamy, 2006. Sensitivity study of Gaussian dispersion models. J. Sci. Ind. Res., 65: 321-324.

Turner, D.B., 1997. The long lifetime of the dispersion methods of Pasquill in U.S. regulatory air modeling. J. Applied Meteorol., 36: 1016-1020.

Vosloo, W.L., 2002. A comparison of the performance of high-voltage insulator materials in a severely polluted coastal environment. Ph.D Thesis, Stellenbosch University, Stellenbosch, South Africa.

Zhang, R., A.F. Khalizov, J. Pagels, D. Zhang and H. Xue *et al*., 2008. Variability in morphology, hygroscopicity and optical properties of soot aerosols during atmospheric processing. Proc. National Acad. Sci., 105: 10291-10296.

Zhicheng, Z., Q. Deli, C. Xinhao, R. Xia and Z. Xuefei, 2015. Preliminary assessment of numerical simulation of atmospheric particulate matter causing pollution flashover of grid equipments. Proceedings of the 12th International Computer Conference on Wavelet Active Media Technology and Information Processing (ICCWAMTIP), December, 18-20, 2015, IEEE, Chengdu, China ISBN:978-1-4673-8266-3, pp: 487-492.